applied sciences

MDPI

Article

Improvement of Light Extraction in Deep Ultraviolet GaN Light Emitting Diodes with Mesh P-Contacts

Shiou-Yi Kuo, Chia-Jui Chang, Zhen-Ting Huang and Tien-Chang Lu *

Department of Photonics and Institute of Electro-Optical Engineering, College of Electrical and Computer Engineering, National Chiao Tung University, 1001 Ta Hsueh Rd., Hsinchu 300, Taiwan; hughkuo.eo04g@nctu.edu.tw (S.-Y.K.); chiajui.eo08g@nctu.edu.tw (C.-J.C.); zzxxj28395.eo07g@nctu.edu.tw (Z.-T.H.)

* Correspondence: timtclu@mail.nctu.edu.tw

Received: 14 July 2020; Accepted: 17 August 2020; Published: 21 August 2020

Abstract: One of the main reasons that the emission efficiency of GaN-based light-emitting diodes (LEDs) decreases significantly as the emission wavelength shorter than 300 nm is the low light extraction efficiency (LEE). Especially in deep ultra-violet (DUV) LEDs, light propagating outside the escape cone and being reflected back to the semiconductor or substrate layer is absorbed not only by active layers but also by p-type layers with narrower bandgaps and electrodes that are neither transparent nor reflective of the DUV wavelength. In this report, we propose a DUV LED structure with mesh p-GaN/indium-tin-oxide (ITO) contacts and a Ti/Al/Ni/Au layer as a reflective layer to improve LEE. The mesh p-GaN/ITO DUV LED showed an output power of 12% higher than that from the conventional DUV LED due to the lower light absorption at 280 nm.

Keywords: LED; DUV; LEE; ITO

1. Introduction

Light-emitting diodes (LEDs) have rapidly developed into the main light source in the world because of the high emission efficiency of the blue band from InGaN/GaN multiple quantum wells (MQWs) grown on sapphire substrates [1–6]. Although there is some controversy about the decline in the efficiency of blue GaN LEDs, under certain controlled operating conditions, the state-of-the-art external quantum efficiency (EQE) has reached approximately 75% [7]. The GaN material system exhibits fascinating characteristics. The AlInGaN alloy composition can be adjusted to control its emission wavelength. In principle, the emission wavelength corresponding to the bandgap of the alloy can be tuned from the infrared (IR), visible to ultraviolet (UV) bands [8,9]. However, when the emission wavelength is adjusted to the green and ultraviolet bands, the emission efficiency of GaN-based LEDs rapidly decreases. There are many reasons for the rapid decline, including immature epitaxial growth and process technology [10–15]. The reason why AlGaN-based UV LEDs' technology becomes important is that people see that the application of UV LEDs is of great help to our daily lives. We can simply subdivide UV into UVA, UVB, and UVC. UVA (Near-UV light source) is the wavelength range of 365 nm to 410 nm. UVC is the wavelength range of 200 nm to 280 nm, also called deep ultraviolet (DUV) light, with the advantages of short wavelength and high energy. It can destroy the molecular structure and function of nucleic acids in the cells of microorganisms (bacteria, viruses, spores, and other pathogens) through radiation in a short time and the microbial cells are lethal and cannot be regenerated to achieve the purpose of disinfection and sterilization. Therefore, the DUV LED is widely used in medical phototherapies, such as air sterilization and purification, water sterilization (including static water and flowing water), and surface disinfection [16–18].

The efficiencies and power levels of AlGaN-based UV LEDs today are still low compared to visible wavelengths, such as blue, green, and red LEDs [19]. The main reasons for low EQE is the low light-extraction efficiency (LEE). Many LED structures have improved the LEEs by using pattern sapphire substrates [20,21], different designs of chip structures [22–24], and different reflective materials of p-side mirrors [25,26]. Especially in DUV LEDs, light propagating outside the escaping cone formed by the refractive index contrast between the chip and the environment, and that is reflected back to the semiconductor and substrate layer, will be absorbed by active layers, p-type layers with smaller bandgaps and electrodes that have low reflectivity to the wavelength of the DUV. Different designs of p-side structures and mirror systems have been shown to enhance light output from near-UV LEDs [27–30]. In this study, we propose a DUV LED structure with mesh p-GaN/indium-tin-oxide (ITO) contacts and a Ti/Al/Ni/Au layer as a reflective layer to improve LEE. By carefully arranging the mesh configuration, we can significantly improve the emission efficiency and increase the output power of the DUV LED with an emission wavelength at 280 nm.

2. Materials and Methods

In this work, trimethylgallium (TMGa), trimethylaluminum (TMAl) for the group-III element, and ammonia (NH_3) for the group-V element were used in the low-pressure metal-organic chemical vapor deposition (MOCVD) to grow the DUV LED structure on an AlN template grown (0001)-oriented c-plane sapphire substrate. Firstly, a 25 nm-thick AlN template was grown as a buffer layer followed by a 1.5 µm-thick AlN layer, and a 2 µm-thick Si-doped $Al_{0.45}Ga_{0.55}N$ layer. Then, five periods of Si-doped $Al_{0.4}Ga_{0.6}N/Al_{0.6}Ga_{0.4}N$ Multiple Quantum Well (MQW)s comprising 6 nm-thick Si-doped $Al_{0.4}Ga_{0.6}N$ quantum wells and 6 nm-thick Si-doped $Al_{0.6}Ga_{0.4}N$ barriers were grown on the Si-doped $Al_{0.45}Ga_{0.55}N$. Finally, 20 nm-thick p-$Al_{0.7}Ga_{0.3}N$ layer electron blocking layers (p-EBLs) doped with Mg were grown, followed by a 50 nm-thick p-$Al_{0.3}Ga_{0.7}N$ layer and a 50 nm-thick p-GaN for the current spreading contact layer. The carrier concentrations were estimated to be 4×10^{18} cm^{-3} in the n-AlGaN layer by the Hall measurement. The doping concentration of Mg in p-GaN was estimated to be 8×10^{18} cm^{-3}. The schematic layer structure of the based-DUV LEDs is shown as Figure 1a. The chip process begins with the use of inductively coupled plasma (ICP) etching to define a 510 µm × 510 µm mesa with an array of a circular recess having a diameter of 40 µm for n-contacts. For n-ohmic-contact electrodes, a stack of Ti/Al/Ti/Au layers was deposited by electron beam (E-beam) evaporation and then alloyed at 800 °C for 180 s in an N_2 atmosphere to reduce the contact resistance.

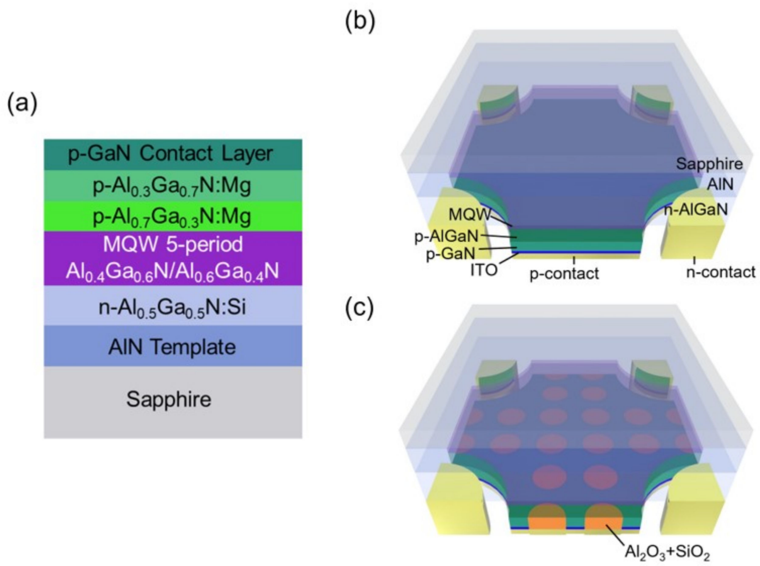

Figure 1. (**a**) The schematic epi-structure of based-DUV LEDs- Deep Ultraviolet. (**b**) The schematics of the conventional DUV LED. (**c**) The schematics of the mesh p-GaN/ITO DUV LED within four n-contacts.

After that, two kinds of p-ohmic-contact structures were fabricated for comparison. The conventional DUV LED was deposited with an ITO layer by the sputtering system on the p-GaN layer as the p-ohmic-contact layer, and a stack of Ti/Al/Ni/Au was deposited by the E-beam evaporation on the ITO layer as a reflective layer. However, the DUV attenuation coefficients in the p-GaN and ITO are large, which will lead to low light efficiency. In order to improve this situation, the mesh p-GaN/ITO structure was proposed and formed by etching in the ITO layer and P-GaN layer of the DUV LED, and formed an array of circular holes with a diameter of 9 µm. Next, an Al_2O_3 layer (50 nm) deposited by atomic layer deposition (ALD) and a SiO_2 layer (50 nm) deposited by plasma-enhanced chemical vapor deposition (PECVD) were applied as the passivation layer to cover the sidewalls of these circular holes from the leakage current. Similarly, the reflective layer was deposited on the ITO layer. The novel structure reduces the volume of the p-GaN layer and ITO layer, which can decrease the light absorption in the chip. Figure 1b,c are three-dimensional schematic views of the conventional DUV LED and the mesh p-GaN/ITO DUV LED within four n-contacts.

For more accurate measurements, we did the packaging process of the conventional DUV LED and the mesh p-GaN/ITO DUV LED. We placed packages of the two structures into an integrating sphere with Instrument Systems CAS 140CT to measure the light output intensity-current (L–I) characteristics, the current-voltage (I–V) characteristics, and the emission spectra of the two structures. We used the Ophir SP620U beamview measurement system to measure the emission patterns of the two structures.

3. Results

Figure 2 shows the optical microscope (OM) and scanning electron microscope (SEM) images of the mesh p-GaN/ITO DUV LED. In Figure 2a, the OM image is taken from the substrate side. Large circular array and smaller circular mesh are n-contacts and holes in the p-GaN/ITO layers, respectively. In Figure 2b, the SEM image is taken from the p-side. The two large pads are for bonding with the n and p electrodes. The mesh holes in the p-GaN/ITO layers are colored with blue. Figure 2c is the enlarged SEM image of the area marked by a red rectangular dashed box in Figure 2b. We cut the sample along the dashed line shown in Figure 2c on the p-contacts and the corresponding cross-sectional image is shown in Figure 2d. We can clearly see that the p-GaN/ITO was etched down by 50 nm, and the passivation layer indeed covered the sidewalls of the p-GaN layer. To further improve the characteristics of the DUV LEDs, the mesh p-GaN/ITO structures were investigated.

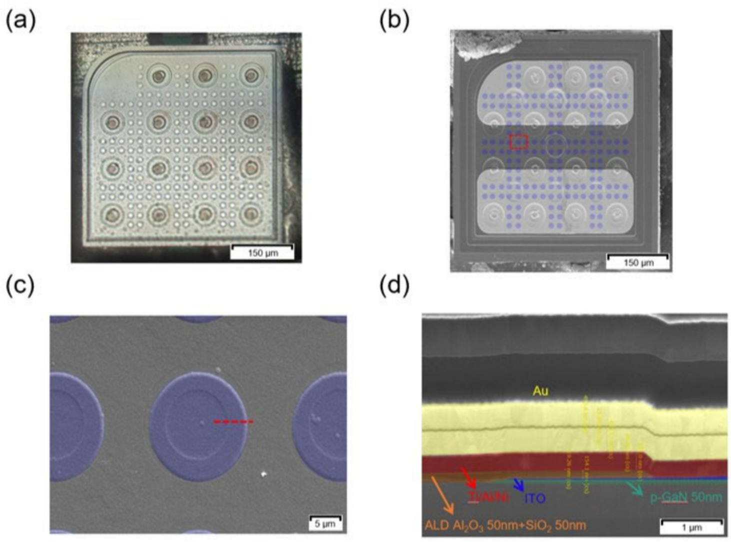

Figure 2. The OM and SEM images of the mesh p-GaN/ITO DUV LED. (**a**) OM image taken from the substrate side (**b**) SEM image taken from the p-side. (**c**) Enlarge SEM image of mesh p contact (**d**) Cross-sectional image of mesh p contact.

Figure 3a shows the light output L–I characteristics and the I–V characteristics of two kinds of DUV LEDs. The mesh p-GaN/ITO DUV LED shows the output power of approximately 5.64 mW at 20 mA, which is 12% higher than the output power from the conventional DUV LED. The improvement of light output emission may result from the novel structure that reduces the volume of the P-GaN layer and the ITO layer, which can decrease the light absorption in the chip. The mesh p-GaN/ITO DUV LED shows the voltage of approximately 6.65 V at 20 mA, which is higher than the voltage of the conventional DUV LED due to the smaller contact area. Figure 3b shows External Quantum Efficiency (EQE) versus the current characteristics and the emission spectra of the two kinds of DUV LED. The EQE is defined by the ratio of the number of emitted photons to the number of electrons injected into the device, and can be calculated by the output power divided by the input current multiplied with the photon energy to the electronic charge ratio. The mesh p-GaN/ITO DUV LED showed that the EQE value was as high as 6.3% at 20 mA. In addition, the notorious efficiency droop was not observed up to 120 mA and the output power could reach 32 mW at 120 mA. The wavelength peaks of the two kinds of DUV LED were almost the same, which were at 280 nm, and the intensity of the mesh p-GaN/ITO DUV LED was higher than the one for the conventional DUV LED.

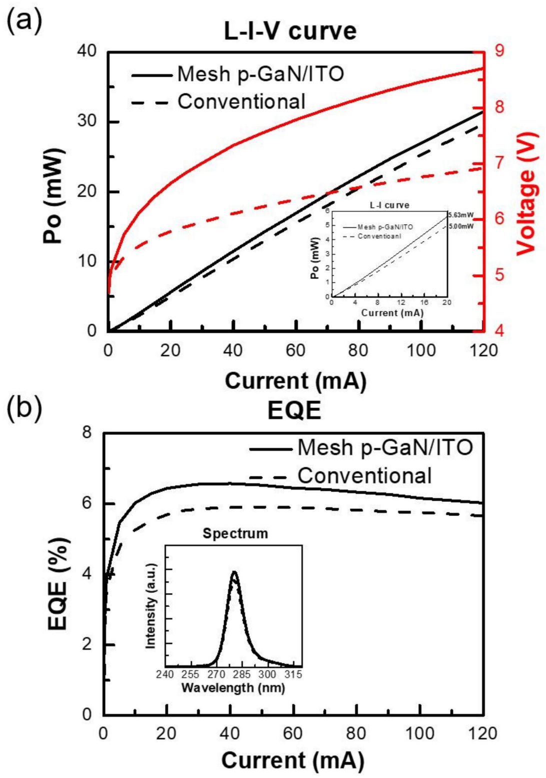

Figure 3. (**a**) The measured L–I characteristics and I–V characteristics of the two kinds of DUV LEDs. The inset shows L-I characteristics from 0 to 20 mA. (**b**) EQE versus current characteristics of the two kinds of DUV LED. The inset shows the emission spectra of the two kinds of DUV LEDs. The solid line and dashed lines are data curves for the mesh p-GaN/ITO DUV LED and the conventional DUV LED.

Figure 4a,b show near field light emission patterns observed by the beam view measurement system for the two kinds of the DUV LEDs at 20 mA. The beam view patterns generally reveal the output power and carrier distribution. As a consequence, different p-layer structure design makes different beam view results. The beam view of the mesh p-GaN/ITO DUV showed a higher output emission pattern on the area with p-GaN/ITO. The results clearly indicated that light output intensity would be greatly improved by reducing light absorption in the chip.

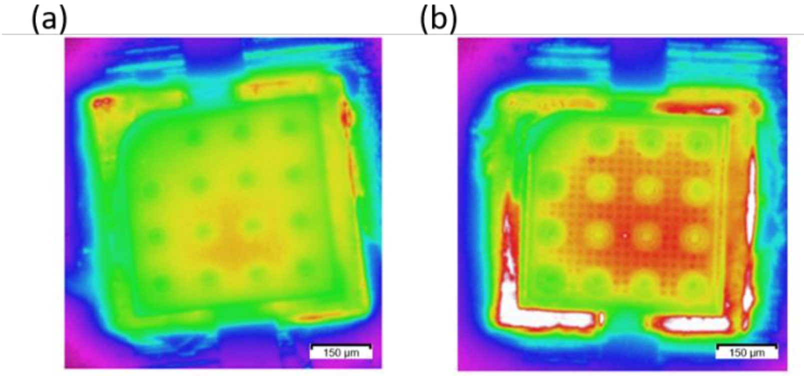

Figure 4. Near field light emission patterns of (**a**) the conventional DUV LED and (**b**) the mesh p-GaN/ITO DUV LED.

4. Discussion

In order to study the effect and design of p-mesh contacts for DUV LEDs, simplified 2D simulations were executed with Advanced Physical Models of Semiconductor Devices (APSYS) simulation program from Crosslight Software, Inc, which can deal with electrical and optical properties of LEDs. There are four structures to be compared: conventional ones (unmeshed) and three meshed ones with the same remained p-GaN area but meshed into 2, 3, and 4 segments, respectively [31,32]. The detailed structural parameters are shown in Figure 5a. The model only deals with the region between two n-contacts similar to the schematics shown in Figure 1. In the simulation, the Shockley–Read–Hall recombination lifetime, zBN, and Auger recombination coefficient were set to be 3 ns, 8×10^{-13} cm^2/s, 1×10^{-30} cm^6/s, respectively [28,29]. The polarization screening coefficient and carrier mobility are tuned to fit the I–V curve of conventional one obtained from the experiment, which has a turn-on voltage of 5.5 V and a serial resistance of about 85 Ω. For different absorption behavior of the four structures, ray-tracing simulations are conducted to acquire the light extraction efficiency. The light sources in the ray-tracing simulations are set according to the distribution of radiative recombination, and the absorption coefficients of p-GaN and ITO are set to be 1.7×10^5 cm^{-1} and 1×10^5 cm^{-1} while the other regions are assumed to be transparent [33,34].

Figure 5b shows the simulated L–I–V characteristics and the extraction efficiencies of the four structures, which are 37.1%, 43.6%, 41.2%, and 42.6%, respectively. Indeed, the light extraction efficiency improved by 15–17% when the p-GaN and ITO layers were meshed; however, no obvious variations of extraction efficiencies were observed when further dividing those layers into more segments. On the other hand, a monotonic increase of operating voltage was observed with the increase of segments number, and the large operating voltage caused an unbalanced MQW band diagram leading to much severe electron current leakage. Figure 5c shows the normalized electron current flowing in the growth direction, and the electron current flowing through the active region was considered to be a leakage current. It is noteworthy that, the current was not uniform over lateral direction, so the electron current in Figure 5c was the integrated result to reflect the overall condition. In Figure 5c, nearly 100% of the electron flies over the active region, which explains the unusual low output power of the four-segment structure. The leakage current effect was less severe in the three-segment structure and it showed much better light output power. Although the leakage current effect in the two-segments structure was a little bit higher than that in the unmeshed structure, the fewer light absorption in p-GaN and ITO, as well as the light scattering effect, make the light output power of the two-segment structure higher than that of the unmeshed structure, and the results were consistent with the experimental ones.

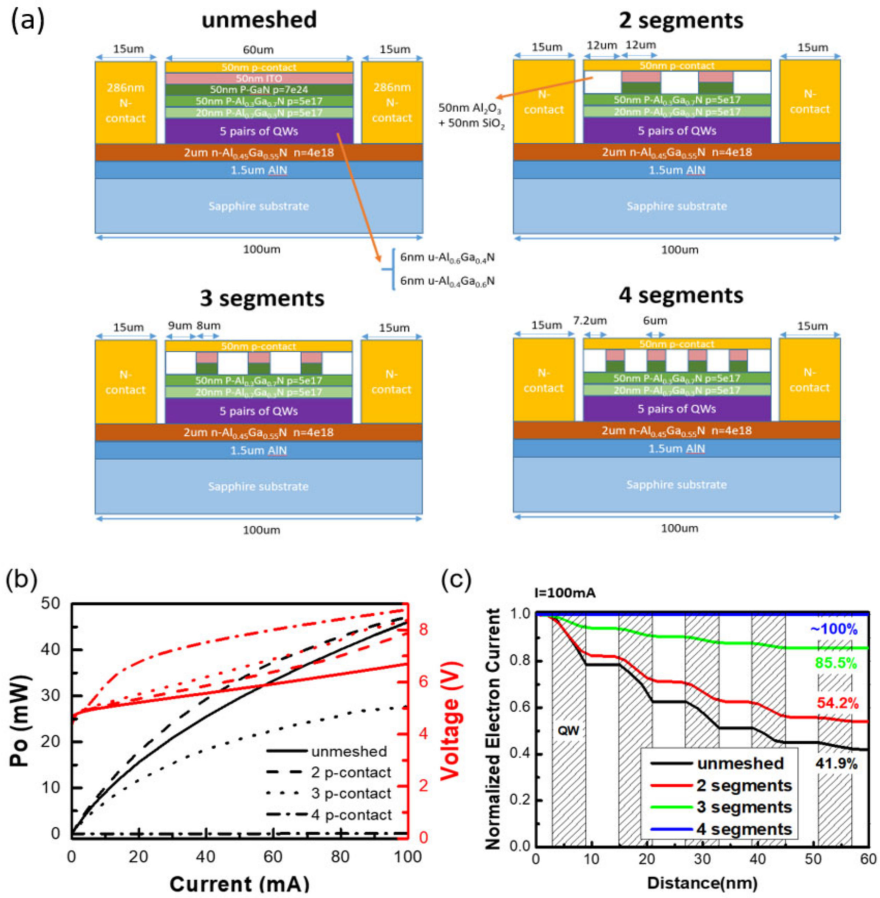

Figure 5. (**a**) Schematic diagrams of the simulated structures. (**b**) Simulated L–I–V characteristics of the four structures. (**c**) Normalized electron current in the active region.

5. Conclusions

We have fabricated DUV LED structures with the mesh p-GaN/ITO structure. Thanks to the lower light absorption at 280 nm, the mesh p-GaN/ITO DUV LED showed a 12% output power enhancement compared to the conventional DUV LED. The EQE value was as high as 6.3% at 20 mA. In addition, the notorious efficiency droop was not observed up to 120 mA, and the output power reached 32 mW at 120 mA. We also employed a simple 2D simulation model to study the optimum p-mesh contact structure, and revealed the balance between the light absorption and leakage current due to the high voltage. These improvements should facilitate highly efficient solid state DUV light sources penetrating into important health applications such as purification, disinfection, and sterilization.

Author Contributions: Conceptualization, S.-Y.K.; methodology, S.-Y.K., C.-J.C., Z.-T.H., and T.-C.L.; software, C.-J.C.; validation, S.-Y.K., C.-J.C., Z.-T.H.; formal analysis; S.-Y.K., C.-J.C., Z.-T.H.; resources, T.-C.L.; writing, S.-Y.K., C.-J.C., Z.-T.H.; visualization, Z.-T.H. and T.-C.L.; supervision, T.-C.L.; project administration, T.-C.L.; funding acquisition, T.-C.L. All authors have read and agreed to the published version of the manuscript.

Funding: This research was funded by Ministry of Science and Technology (MoST) of Taiwan, under the project number MOST 109-2124-M-009-005.

Acknowledgments: The authors would like to gratefully acknowledge Semiconductor Laser Laboratory, Nano Facility Center and Nano Device Laboratories for technical support.

Conflicts of Interest: The authors declare no conflict of interest.

References

1. Nakamura, S.; Senoh, M.; Mukai, T. High-Power InGaN/GaN double-heterostructure violet light emitting diodes. *Appl. Phys. Lett.* **1993**, *62*, 2390–2392. [CrossRef]
2. Chichibu, S.F.; Abare, A.C.; Minsky, M.S.; Keller, S.; Fleischer, S.B.; Bowers, J.E.; Hu, E.; Mishra, U.K.; Coldren, L.A.; DenBaars, S.P.; et al. Effective band gap inhomogeneity and piezoelectric field in InGaN/GaN multiquantum well structures. *Appl. Phys. Lett.* **1998**, *73*, 2006–2008. [CrossRef]
3. Simon, J.; Protasenko, V.; Lian, C.; Xing, H.; Jena, D. Polarization induced hole doping in wide-band-gap uniaxial semiconductor heterostructures. *Science* **2010**, *327*, 60–64. [CrossRef] [PubMed]
4. Goepfert, I.D.; Schubert, E.F.; Osinsky, A.; Norris, P.E.; Faleev, N.N. Experimental and theoretical study of acceptor activation and transport properties in p-type AlxGa1-x N/GaN superlattices. *J. Appl. Phys.* **2000**, *88*, 2030–2038. [CrossRef]
5. Lee, Y.; Hwang, J.; Hsu, T.; Hsieh, M.; Jou, M.; Lee, B.J.; Lu, T.-C.; Kuo, H.C.; Wang, S. GaN-Based LEDs with Al-deposited V-shaped sapphire facet mirror. *IEEE Photonics Technol. Lett.* **2006**, *18*, 724–726. [CrossRef]
6. Wang, C.H.; Ke, C.C.; Lee, C.Y.; Chang, S.P.; Chang, W.T.; Li, J.C.; Li, Z.Y.; Yang, H.C.; Kuo, H.-C.; Lu, T.-C.; et al. Hole injection and efficiency droop improvement in InGaN/GaN light-emitting diodes by band-engineered electron blocking layer. *Appl. Phys. Lett.* **2010**, *97*, 261103. [CrossRef]
7. Cich, M.J.; Aldaz, R.I.; Chakraborty, A.; David, A.; Grundmann, M.J.; Tyagi, A.; Zhang, M.; Steranka, F.; Krames, M.R. Bulk GaN based violet light-emitting diodes with high efficiency at very high current density. *Appl. Phys. Lett.* **2012**, *101*, 223509. [CrossRef]
8. Streubel, K.; Jaeger, A.; Linder, N.; Wirth, R. High brightness AlGaInP light-emitting diodes. *IEEE J. Sel. Top. Quantum Electron.* **2002**, *8*, 321–332. [CrossRef]
9. Nakamura, S.; Senoh, M.; Iwasa, N.; Nagahama, S.-I. High-Power InGaN single-quantum-well-structure blue and violet light-emitting diodes. *Appl. Phys. Lett.* **1995**, *67*, 1868–1870. [CrossRef]
10. Zhao, H.; Liu, G.; Zhang, J.; Poplawsky, J.D.; Dierolf, V.; Tansu, N. Approaches for high internal quantum efficiency green InGaN light-emitting diodes with large overlap quantum wells. *Opt. Express* **2011**, *19*, A991–A1007. [CrossRef]
11. Chiu, C.; Li, Z.-Y.; Chao, C.; Lo, M.; Kuo, H.-C.; Yu, P.; Lu, T.-C.; Wang, S.; Lau, K.M.; Cheng, S. Efficiency enhancement of UV/blue light emitting diodes via nanoscaled epitaxial lateral overgrowth of GaN on a SiO2 nanorod-array patterned sapphire substrate. *J. Cryst. Growth* **2008**, *310*, 5170–5174. [CrossRef]
12. Liu, W.H.; Chu, C.F.; Cheng, C.C.; Hsu, K.H.; Chung, Y.T.; Wang, Y.K.; Li, C.C.; Chu, J.Y.; Fan, F.H.; Cheng, H.C.; et al. Development of high-power UV LEDs for epoxy curing applications. *Gallium Nitride Mater. Devices V* **2010**, *7602*, 76021K. [CrossRef]
13. Wang, C.; Ke, C.; Chiu, C.; Li, J.; Kuo, H.-C.; Lu, T.-C.; Wang, S. Study of the internal quantum efficiency of InGaN/GaN UV LEDs on patterned sapphire substrate using the electroluminescence method. *J. Cryst. Growth* **2011**, *315*, 242–245. [CrossRef]
14. Ryu, H.-Y.; Choi, I.-G.; Choi, H.-S.; Shim, J.-I. Investigation of Light Extraction Efficiency in AlGaN Deep-Ultraviolet Light-Emitting Diodes. *Appl. Phys. Express* **2013**, *6*, 062101. [CrossRef]
15. Fujioka, A.; Asada, K.; Yamada, H.; Ohtsuka, T.; Ogawa, T.; Kosugi, T.; Kishikawa, D.; Mukai, T. High-Output-Power 255/280/310 nm deep ultraviolet light-emitting diodes and their lifetime characteristics. *Semicond. Sci. Technol.* **2014**, *29*, 084005. [CrossRef]
16. Adivarahan, V.; Fareed, Q.; Islam, M.; Katona, T.; Krishnan, B.; Khan, A. Robust 290 nm Emission Light Emitting Diodes over Pulsed Laterally Overgrown AlN. *Jpn. J. Appl. Phys.* **2007**, *46*, L877–L879. [CrossRef]
17. Kneissl, M.; Kolbe, T.; Chua, C.; Kueller, V.; Lobo, N.; Stellmach, J.; Knauer, A.; Rodriguez, H.; Einfeldt, S.; Yang, Z.; et al. Advances in group III-nitride-based deep UV light-emitting diode technology. *Semicond. Sci. Technol.* **2010**, *26*, 14036. [CrossRef]
18. Hirayama, H.; Maeda, N.; Fujikawa, S.; Toyoda, S.; Kamata, N. Recent progress and future prospects of AlGaN-based high-efficiency deep-ultraviolet light-emitting diodes. *Jpn. J. Appl. Phys.* **2014**, *53*, 100209. [CrossRef]
19. Khan, A.; Balakrishnan, K.; Katona, T. Ultraviolet light-emitting diodes based on group three nitrides. *Nat. Photonics* **2008**, *2*, 77–84. [CrossRef]
20. Bell, A.; Liu, R.; Ponce, F.A.; Amano, H.; Akasaki, I.; Cherns, D. Light emission and microstructure of Mg-doped AlGaN grown on patterned sapphire. *Appl. Phys. Lett.* **2003**, *82*, 349–351. [CrossRef]

21. Wuu, D.S.; Wang, W.; Shih, W.; Horng, R.; Lee, C.; Lin, W.; Fang, J. Enhanced output power of near-ultraviolet InGaN-GaN LEDs grown on patterned sapphire substrates. *IEEE Photonics Technol. Lett.* **2005**, *17*, 288–290. [CrossRef]
22. Morita, D.; Sano, M.; Yamamoto, M.; Murayama, T.; Nagahama, S.-I.; Mukai, T. High Output Power 365 nm Ultraviolet Light Emitting Diode of GaN-Free Structure. *Jpn. J. Appl. Phys.* **2002**, *41*, L1434–L1436. [CrossRef]
23. Cheng, B.-S.; Chiu, C.-H.; Lo, M.-H.; Wu, Y.-L.; Kuo, H.-C.; Lu, T.-C.; Cheng, Y.-J.; Wang, S.-C.; Huang, K.-J. Light Output Enhancement of UV Light-Emitting Diodes with Embedded Distributed Bragg Reflector. *IEEE Photonics Technol. Lett.* **2011**, *23*, 642–644. [CrossRef]
24. Morita, D.; Yamamoto, M.; Akaishi, K.; Matoba, K.; Yasutomo, K.; Kasai, Y.; Sano, M.; Nagahama, S.-I.; Mukai, T. Watt-Class High-Output-Power 365 nm Ultraviolet Light-Emitting Diodes. *Jpn. J. Appl. Phys.* **2004**, *43*, 5945–5950. [CrossRef]
25. Wuu, D.-S.; Hsu, S.-C.; Huang, S.-H.; Wu, C.-C.; Lee, C.-E.; Horng, R.-H. GaN/Mirror/Si Light-Emitting Diodes for Vertical Current Injection by Laser Lift-Off and Wafer Bonding Techniques. *Jpn. J. Appl. Phys.* **2004**, *43*, 5239–5242. [CrossRef]
26. Kim, J.K.; Xi, J.-Q.; Luo, H.; Schubert, E.F.; Cho, J.; Sone, C.; Park, Y. Enhanced light-extraction in GaInN near-ultraviolet light-emitting diode with Al-based omnidirectional reflector having NiZn/Ag microcontacts. *Appl. Phys. Lett.* **2006**, *89*, 141123. [CrossRef]
27. Lobo, N.; Rodriguez, H.; Knauer, A.; Hoppe, M.; Einfeldt, S.; Vogt, P.; Weyers, M.; Kneissl, M. Enhancement of light extraction in ultraviolet light-emitting diodes using nanopixel contact design with Al reflector. *Appl. Phys. Lett.* **2010**, *96*, 81109. [CrossRef]
28. Kashima, Y.; Maeda, N.; Matsuura, E.; Jo, M.; Iwai, T.; Morita, T.; Kokubo, M.; Tashiro, T.; Kamimura, R.; Osada, Y.; et al. High external quantum efficiency (10%) AlGaN-based deep-ultraviolet light-emitting diodes achieved by using highly reflective photonic crystal on p-AlGaN contact layer. *Appl. Phys. Express* **2017**, *11*, 012101. [CrossRef]
29. Maeda, N.; Yun, J.; Jo, M.; Hirayama, H. Enhancing the light-extraction efficiency of AlGaN deep-ultraviolet light-emitting diodes using highly reflective Ni/Mg and Rh as p-type electrodes. *Jpn. J. Appl. Phys.* **2018**, *57*, 04FH08. [CrossRef]
30. Maeda, N.; Jo, M.; Hirayama, H. Improving the Efficiency of AlGaN Deep-UV LEDs by Using Highly Reflective Ni/Al p-Type Electrodes. *Phys. Status Solidi A* **2018**, *215*, 1700435. [CrossRef]
31. Kuo, Y.-K.; Chang, J.-Y.; Chen, F.-M.; Shih, Y.-H.; Chang, H.-T. Numerical Investigation on the Carrier Transport Characteristics of AlGaN Deep-UV Light-Emitting Diodes. *IEEE J. Quantum Electron.* **2016**, *52*, 1–5. [CrossRef]
32. De Santi, C.; Meneghini, M.; Monti, D.; Glaab, J.; Guttmann, M.; Rass, J.; Einfeldt, S.; Mehnke, F.; Enslin, J.; Wernicke, T.; et al. Recombination mechanisms and thermal droop in AlGaN-based UV-B LEDs. *Photonics Res.* **2017**, *5*, A44–A51. [CrossRef]
33. Muth, J.F.; Brown, J.D.; Johnson, M.A.L.; Yu, Z.; Kolbas, R.M.; Cook, J.W.; Schetzina, J.F. Absorption Coefficient and Refractive Index of GaN, AlN and AlGaN Alloys. *MRS Internet J. Nitride Semicond. Res.* **1999**, *4*, 502–507. [CrossRef]
34. Khusayfan, N.M.; El-Nahass, M.M. Study of Structure and Electro-Optical Characteristics of Indium Tin Oxide Thin Films. *Adv. Condens. Matter Phys.* **2013**, *2013*, 1–8. [CrossRef]